J. Phys. Chem. Solids Vol. 54, No. 11, pp. 1533–1542, 1993
Printed in Great Britain.

0022-3697/93 $6.00 + 0.00

OPTICAL PROPERTIES AND UPCONVERTED EMISSIONS OF Tm^{3+} IN Yb^{3+} DOPED FLUOROPHOSPHATE GLASSES

G. ÖZEN, XU WU,† J. P. DENIS, A. KERMAOUI,‡ F. PELLÉ and B. BLANZAT
Laboratoire de Physico-Chimie des Matériaux, C.N.R.S., 1 Place Aristide Briand, 92190 Meudon, France

(*Received* 22 *June* 1993; *accepted* 15 *July* 1993)

Abstract—Optical properties of Tm^{3+} ions in Yb^{3+} doped fluorophosphate glasses containing 27 mole% PbF_2 have been studied. The absorption, luminescence and excitation spectra, and the decay patterns were obtained as function of temperature, TmF_3 and YbF_3 concentrations. For the blue emission centered at 479 nm ($^1G_4 \rightarrow {}^3H_6$ transition) the critical concentration of Tm^{3+} is 0.2 mole% when the concentration of Yb^{3+} is kept constant at 20 mole%. The oscillator strengths of the transitions between J manifolds are calculated by using Judd–Ofelt theory at room temperature and were compared with the ones obtained experimentally. Radiative lifetimes of the excited states are determined and used to obtain nonradiative transition rates and the quantum yields. Upconverted emissions from the $^1D_2$, $^1G_4$ and $^3F_4$ levels were observed when the Yb^{3+} ions were excited with 966 nm light. An absolute upconversion efficiency for the blue (479 nm) and red (791 nm) emissions was obtained using a comparative method at room temperature. The efficiency of the 479 and 791 nm emissions was measured to be 5×10^{-8} and 7×10^{-4}, respectively, for the sample containing 0.2 mole% TmF_3 and 20 mole% YbF_3 upon 966 nm excitation with an absorbed intensity of 20 mW cm^{-2}.

The emission intensity and the decay time of the $^1G_4$ level were found to be independent of temperature although the emission intensity and the decay time of $^3F_4$ level show small temperature dependence when the desired level was directly excited. However, the upconverted emission intensity of these levels depends on temperature. This behaviour may be due to a phonon-assisted energy transfer mechanism from Yb^{3+} to Tm^{3+}.

Keywords: Glass, upconversion, optical properties.

1. INTRODUCTION

The study of luminescence and upconversion processes in crystals and glasses doped with rare earth ions has been attracting great interest [1–3]. The interest arises from the need for higher density in optical data storage and, from the possibility of their application in infrared (i.r.) pumped visible lasers. The recent investigations on heavy metal glasses doped with Er^{3+} [4], Er^{3+}–Yb^{3+} [5] and Tm^{3+}–Yb^{3+} [6] indicated that the efficiency of i.r. to visible conversion of radiation in the glass matrix may be comparable to that obtained in the crystalline matrices [7]. Fluorophosphate glass matrix is one of the promising host materials for the i.r. to visible upconversion lasers. Introducing PbF_2 into the matrix may even increase the upconversion efficiency [8]. Tm^{3+} is one of the possible candidates for obtaining blue laser when introduced in a Yb^{3+} doped glass upon i.r. excitation since $^1D_2$ and $^1G_4$ levels emit blue fluorescence centered at 451 and 479 nm, respectively [9].

In this work, the mechanism of i.r. to visible light (blue and red) conversion was extensively studied in Tm^{3+}, Yb^{3+} codoped fluorophosphate glasses containing 27 mole% PbF_2. To understand what factors control the conversion processes the experimental results were combined with the optical properties of Tm^{3+} obtained by using the Judd–Ofelt theory [10]. The dominant blue emission intensity of $^1G_4$ emission is much stronger than the 451 nm emission of $^1D_2$ level in these glasses upon i.r. excitation. Integrated intensity and dynamics of the luminescence originating from $^1D_2$ and $^1G_4$ levels from which blue upconverted emissions were observed have been studied as a function of Tm^{3+} and Yb^{3+} concentrations and temperature. A similar investigation was also carried out for the red upconverted emission (centered at 791 nm) due to the $^3F_4 \rightarrow {}^3H_6$ transition.

2. EXPERIMENTAL

The samples were prepared by using high purity rare earth fluorides. The general composition of the glass (APbF:RE) is $2.67(AlPO_4) + 37.33(AlF_3) + 27(PbF_2) + (33 - x - y)(CaF_2) + (x)(TmF_3) + (y)(YbF_3)$, where x and y are 0.05, 0.1, 0.2, 0.3, 0.6, 1.0, 1.5 and, 2.0, 5.0, 10, 15, 20, 25, respectively. A small

† Permanent address: Changchun Institute of Physics, Academia Sinica, Changchun, China.
‡ Laboratoire Laser, CDTA 2bd, BP-1017 Alger Gare, Algeria.

amount of $NH_4F.HF$ was also added to the batch. The glasses were obtained by heating the mixture in an aluminum crucible at 900°C for 15 min. The melt was then poured on to a stainless steel plate and pressed with another steel plate. The divitrified glasses were obtained without pressing the melt after the pouring.

The absorption spectra of all the samples were obtained by using a Cary-17 spectrometer at room temperature. The density of the APbF: 20 mole% YbF_3, 1 mole% TmF_3 glass was measured by Archimedes' method to calculate the number of Tm ions per unit volume with the molar weight ($g = 158.4$ g), and is found to be 0.33 mol lt^{-1}. The refractive index, n, of the same sample was measured with Abbe's refractometer and is 1.516.

The luminescence spectra were obtained by exciting the samples with either a 250 W tungsten halogen lamp, passed through an i.r. monochromator and a RG 850 long pass filter or by using a Xe-lamp. The emission from the sample was then focused on the entrance slit of a Jobin–Yvon Model HR1000 scanning monochromator. The signal was detected by a RTC 56 TVP photomultiplier tube (S-20) and the amplified signal with a Takeda Riken model TR8641 amplifier was recorded on a chart recorder.

A CTC-70C cryostat was used for low temperature measurements. The temperature of the sample was changed from 10 to 300 K.

Responses to pulsed excitation measurements were made using either a Molectron dye laser pumped with Sopra Nitrogen laser or GRT flash lamp combined with RG850 long pass filter as the excitation source. The signal detected with a RTC 56 TVP photomultiplier tube was fed to either a PAR 162 boxcar integrator or a Tektronix model 7912AD digitizer combined with a computer.

3. EXPERIMENTAL RESULTS

3.1. *Absorption spectra*

The absorption spectrum of APbF:20 mole% YbF_3, 1 mole% TmF_3 at 300 K is presented in Fig. 1. The bands starting from a longer wavelength correspond to transitions from the ground state, $^3H_6$, to the $^3H_4$, $^3H_5$, $^3F_4$, $^3F_3$, $^3F_2$, $^1G_4$ and $^1D_2$ excited states of Tm^{3+}, respectively. The absorption band of Yb^{3+} due to the $^2F_{7/2} \rightarrow {}^2F_{5/2}$ transition shows three peaks centered at 932, 966 and 975 nm in the sample. The spectra of all the samples are similar. For example, the absorption coefficients of the samples containing 0.2 mole% TmF_3 and 1 mole% TmF_3 were calculated and found to be proportional to the concentration of Tm^{3+} ions. The band positions are in agreement with the previous reports on Tm^{3+} ion in fluorophosphate glasses [8]. Figure 2 represents the energy level diagram of Tm^{3+} and Yb^{3+} ions obtained from the absorption spectrum of APbF:20 mole% YbF_3; 1 mole% TmF_3, and the excitation roots for the upconverted emissions obtained upon i.r. excitation.

The oscillator strengths (f) of the absorption bands were determined experimentally using the following formula:

$$f_{exp} = 4.318 \times 10^{-9} \int \varepsilon(\bar{\nu}) d\nu, \qquad (1)$$

where $\varepsilon(\bar{\nu})$ is the molar extinction coefficient at the mean wavenumber. The oscillator strengths of $^3F_2$ and $^3F_3$ levels are given together since these bands overlap. The f-values for our glass are greater than

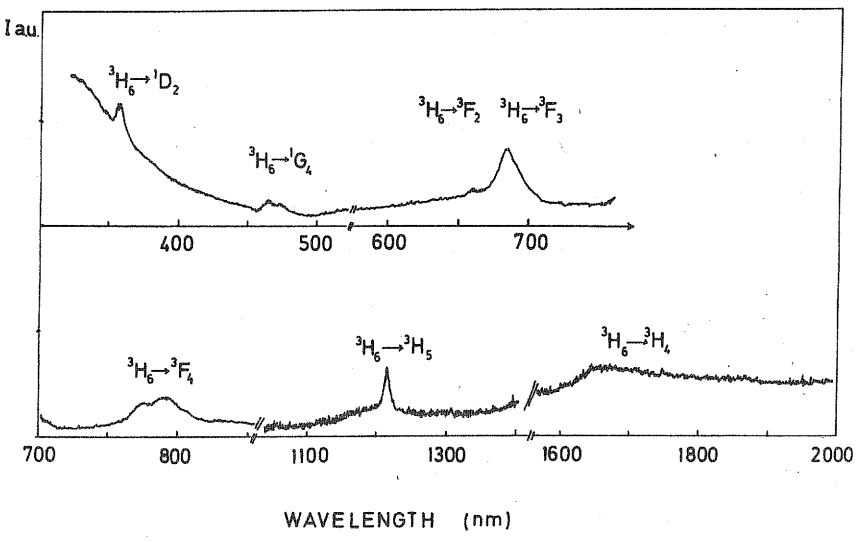

Fig. 1. Absorption spectrum of Tm^{3+} ions in APbF:20 mole% YbF_3 and 1 mole% TmF_3 at room temperature.

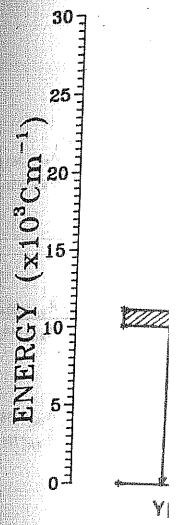

Fig. 2. Energy level di
from the absorption s
and 1 mole% T

those obtained in flu
not contain PbF_2 [8].

The Judd–Ofelt the
f, of a transition fron
state [10, 11]. If the t
the calculated oscillat
transition from the g
cited state ($|S'L'J'\rangle$)

$$f_{cal}(J, J') = \frac{8\pi^2 mc}{3h}$$

where $\bar{\nu}$ is the mean w
cm^{-1}, n is the refractiv
of the ground state
elements, $U(t)$, are nc
have used the values c
LaF_3. The three Judc
obtained by the least sq
tal oscillator strength
and were found to
$\Omega_6 = 1.5 \times 10^{-20}$ cm^2.

Table 1. M
containing

Level
$^1D_2$
$^1G_4$
$^3F_2$
$^3F_3$
$^3F_4$
$^3H_5$
$^3H_4$

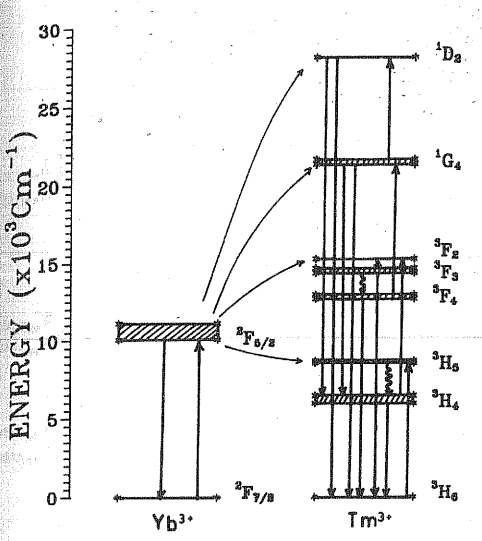

Fig. 2. Energy level diagram of Tm^{3+} and Yb^{3+} obtained from the absorption spectrum of APbF:20 mole% YbF_3 and 1 mole% TmF_3 at room temperature.

those obtained in fluorophosphate glass which does not contain PbF_2 [8].

The Judd–Ofelt theory gives the oscillator strength, f, of a transition from the ground state to an excited state [10, 11]. If the transition is electric dipole type the calculated oscillator strength for an electric dipole transition from the ground state ($\langle SLJ|$) to an excited state ($|S'L'J'\rangle$) is given by

$$f_{cal}(J,J') = \frac{8\pi^2 mc}{3h}\frac{(n^2+2)^2}{9n}\frac{\bar{\nu}^3}{(2J+1)}\sum_{t=2,4,6}\Omega_t(\langle SLJ\|U^{(t)}\|S'L'J'\rangle)^2, \quad (2)$$

where $\bar{\nu}$ is the mean wavenumber of the transition in cm^{-1}, n is the refractive index and J is the degeneracy of the ground state. Since the reduced matrix elements, $U(t)$, are not strongly host-dependent we have used the values calculated by Kaminskii [12] in LaF_3. The three Judd–Ofelt parameters, Ω_t, were obtained by the least squares fitting of our experimental oscillator strength to the $|U^{(t)}|$ matrix elements and were found to be $\Omega_2 = 1.3$, $\Omega_4 = 1.0$ and $\Omega_6 = 1.5 \times 10^{-20}\,cm^2$.

The theoretical f-values were then determined using eqn (2). Measured and calculated oscillator strengths are presented in Table 1. The r.m.s. deviation of the f-calculated from the f-measured values was calculated from the residuals (see Table 1). It is found to be 4.4×10^{-7} which is comparable to the r.m.s. deviation obtained for other glasses [13, 14].

The spontaneous emission probability for a $SLJ \rightarrow S'L'J'$ electric dipole emission is calculated from the following equation:

$$A(J,J') = \frac{64\pi^4 e^2}{3(2J+1)h}\frac{n(n^2+2)^2\bar{\nu}^3}{9}\sum_{t=2,4,6}\Omega_t(\langle SLJ\|U^{(t)}\|S'L'J'\rangle)^2. \quad (3)$$

The total spontaneous emission probability, W_R, for an i^{th} excited state is given as the sum of the $A(J,J')$ terms calculated over all terminal states which is related to the radiative lifetime τ_R and the branching ratios, β, of the level by

$$\frac{1}{\tau_R(i)} = \sum_j A(i,j) = W_R; \text{ and } \beta = \frac{A(J,J')}{W_R}. \quad (4)$$

One of the important parameters for the lasing efficiency of the rare earth ion is the quantum efficiency of the emitting level which is given in [15] by $\eta = \tau/\tau_R$, where τ and τ_R are the measured and the radiative lifetime of the level. Table 2 presents the calculated emission probabilities, radiative lifetime and the branching ratios of the excited states of Tm^{3+} in APbF:20 mole% YbF_3 glass for the electric dipole transitions. Branching ratio of $^1D_2 \rightarrow {}^3H_4$, $^1G_4 \rightarrow {}^3H_6$ and $^3F_4 \rightarrow {}^3H_6$ transitions are 42, 33 and 91%, respectively. These values define the quantum efficiency of each transition which is important for the laser emission.

3.2. *Luminescence and response to pulsed excitation*

3.2.1. *Direct excitation.* The luminescence spectrum of APbF:20 mole% YbF_3, 1 mole% TmF_3 sample was obtained by exciting Tm^{3+} ions into $^1D_2$ and $^1G_4$ levels. The spectra are presented in Fig. 3.

Table 1. Measured and calculated oscillator strengths of Tm^{3+} in fluorophosphate glass containing 20 mole% YbF_3 and 27 mole% PbF_2 at 300 K. All transitions are from the $^3H_6$ level to the level indicated

Level	Wavelength (nm)	Average frequency (cm^{-1})	Oscillator strength (10^{-8}) Measured	Calculated	Residual (10^{-8})
$^1D_2$	356	27,933	136	147	−11
$^1G_4$	470	21,276.6	97	38.6	−58.4
$^3F_2$	659	15,174.5	334	325.2	−8.8
$^3F_3$	686	14,577	334	325.2	−8.8
$^3F_4$	785	12,738.9	172	188.2	16.2
$^3H_5$	1189.4	8407.5	—	—	—
$^3H_4$	1714	5834.3	117	120.2	3.2

Table 2. Calculated spontaneous emission probabilities of Tm^{3+} in fluorophosphate glass containing 20 mole% YbF_3 and 27 mole% PbF_2

Transition	Average frequency (cm^{-1})	A_{ed} (s^{-1})	τ_R (ms)	β (ms)
$^1D_2 \rightarrow {}^3H_6$	27,933	4697.9	0.0907	0.426
$^3H_4$	22,098.7	4526.5		0.411
$^3H_5$	19,498.7	90.9		0.008
$^3F_4$	15,194.1	837.0		0.076
$^3F_3$	13,355.7	338.3		0.031
$^3F_2$	12,758.5	396.8		0.036
$^1G_4$	6656.4	59.0		0.005
$^1G_4 \rightarrow {}^3H_6$	21,276.6	377.8	0.867	0.328
$^3H_4$	15,442.3	115.1		0.100
$^3H_5$	12,869.1	486.4		0.422
$^3F_4$	8537.8	125.3		0.109
$^3F_3$	6699.3	40.6		0.035
$^3F_2$	6102.1	8.3		0.007
$^3F_2 \rightarrow {}^3H_6$	15,174.5	632.1	1.002	0.633
$^3H_4$	9340.2	190.7		0.191
$^3H_5$	6767.0	170.5		0.171
$^3F_3 \rightarrow {}^3H_6$	14,577.3	1677.0	0.548	0.918
$^3H_4$	8743.4	56.0		0.031
$^3H_5$	6169.8	93.6		0.051
$^3F_4 \rightarrow {}^3H_6$	12,738.9	673.1	1.354	0.912
$^3H_4$	6904.6	54.1		0.073
$^3H_5$	4331.4	11.3		0.015
$^3H_4 \rightarrow {}^3H_6$	5834.3	97.7	10.225	1.000

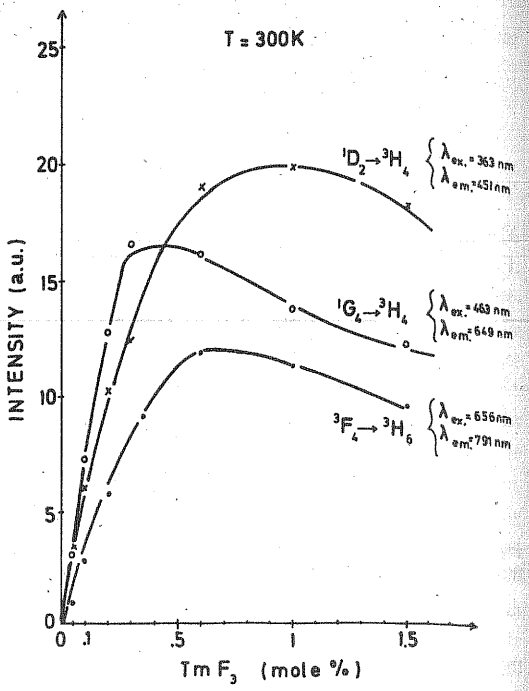

Fig. 4. Integrated intensity of $^1D_2$, $^1G_4$ and $^3F_4$ levels as a function of Tm^{3+} concentration at room temperature.

Three emissions centered at 451, 648, 791 nm, due to the $^1D_2 \rightarrow {}^3H_4$, $^1D_2 \rightarrow {}^3F_4$, and $^1D_2 \rightarrow {}^3F_3$ transitions, were observed if the excitation was into the $^1D_2$ level. No emission originating from the $^1G_4$ level was observed upon this excitation. This indicates that the probability of $^1D_2 \rightarrow {}^1G_4$ transition is small in this glass as predicted from the Judd–Ofelt theory (see Table 2). When the $^1G_4$ level was excited only two bands centered at 649 and 800 nm were observed corresponding to the $^1G_4 \rightarrow {}^3H_4$ and $^3F_4 \rightarrow {}^3H_6$ transitions. The relative intensity of each emission originating from the same level is in agreement with the branching ratio of the transition responsible. For example, the integrated intensity ratio of the 451 nm emission ($^1D_2 \rightarrow {}^3H_4$ transition) to the 648 nm emission ($^1D_2 \rightarrow {}^3F_4$ transition) was measured to be 47 from the emission spectrum obtained upon direct excitation of $^1D_2$ level. This value has been calculated

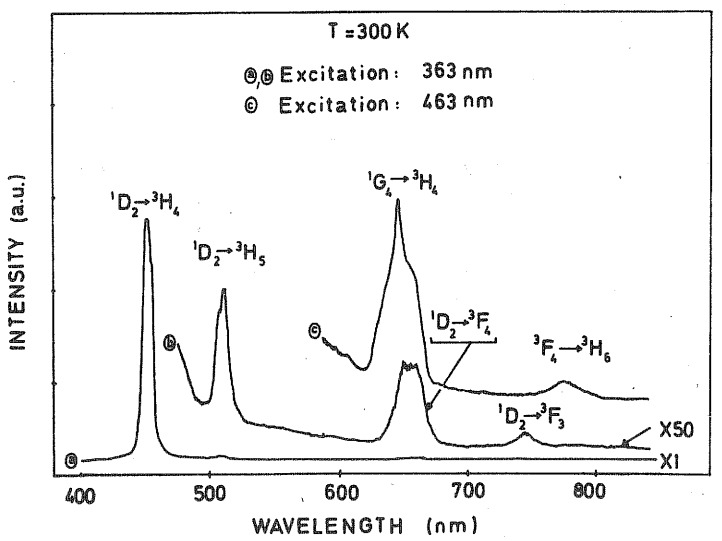

Fig. 3. Emission spectra of APbF:20 mole% YbF_3 and 0.2 mole% TmF_3 at room temperature upon direct excitation. (a) and (b): Excitation was into the $^1D_2$ and $^1G_4$ levels of Tm^{3+} with the Xe-lamp monitored at 363 and 465 nm, respectively.

Fig. 5. Inte

to be 51 from the b
Judd–Ofelt theory.
Figure 4 presents
and $^3F_4$ levels as a
when each level wa
a weak self-quench
tration. The intensi
Tm concentration
concentration is ab
$^3F_4$ level. The quen
slightly stronger tha
the emission of $^3F_4$ l

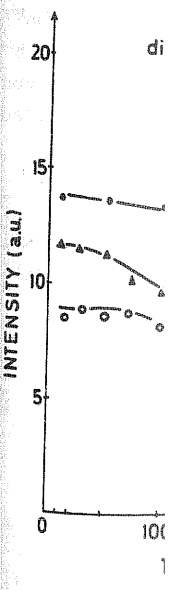

Fig. 6. Temperature de
sions of Tm^{3+} in APb
TmF_3 up

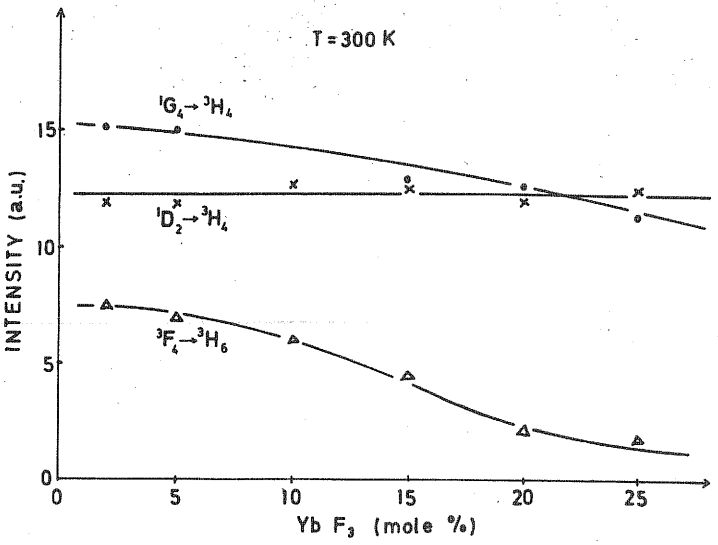

Fig. 5. Integrated intensity of $^1D_2$, $^1G_4$ and $^3F_4$ levels as a function of Yb^{3+} concentration at room temperature.

to be 51 from the branching ratios obtained using the Judd–Ofelt theory.

Figure 4 presents the emission intensity of $^1D_2$, $^1G_4$ and $^3F_4$ levels as a function of Tm^{3+} concentration when each level was excited directly. $^1D_2$ level shows a weak self-quenching above 1 mole% Tm concentration. The intensity of $^1G_4$ emission increases with Tm concentration until 0.2 mole%, while the critical concentration is about 0.6 mole% for the emission of $^3F_4$ level. The quenching of $^1G_4$ level by Tm is only slightly stronger than that for the $^3F_4$ level. However, the emission of $^3F_4$ level is strongly quenched by Yb^{3+} than that of $^1G_4$ level as can be seen in Fig. 5. The effect of Yb^{+3} on $^1D_2$ emission is weak indicating that the coupling of this level with Yb^{3+} ions is negligible.

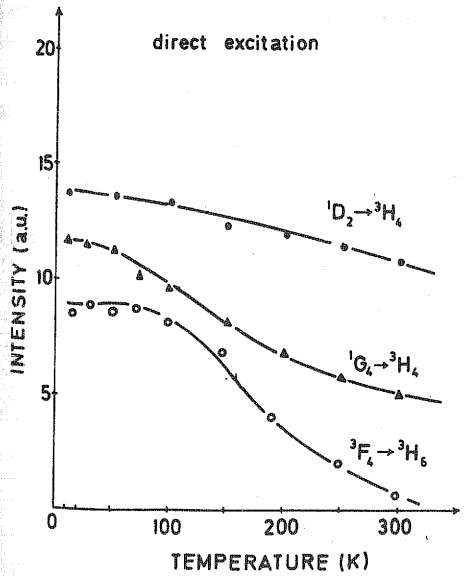

Fig. 6. Temperature dependence of $^1D_2$, $^1G_4$ and $^3F_4$ emissions of Tm^{3+} in APbF:20 mole% YbF_3 and 0.2 mole% TmF_3 upon direct excitation.

Figure 6 shows the effect of temperature on the emissions from $^1D_2$, $^1G_4$ and $^3F_4$ in the range of 11–300 K. Emission of the latter level stays constant below 100 K and starts decreasing rapidly above this temperature. Emission of $^1G_4$ level exhibits a small change up to 40 K and it decreases slowly to less than 40% of its value at 11 and 300 K. The intensity of $^1D_2$ emission is independent of temperature.

The lifetime of $^1D_2$, $^1G_4$ and $^3F_4$ levels was measured by exciting each level directly. The results are presented in Fig. 7 and Table 3 for different concentrations of Tm. The decay pattern of each level consists of two exponential decays in all samples. Time constants for each curve were obtained by fitting the curves with two exponential decays.

The lifetimes of $^1G_4$ and $^3F_4$ levels were also measured as function of temperature from 11 to 300 K to study the effect of temperature on the nonradiative relaxation processes and also on the quantum efficiency. The results are depicted in Fig. 8. Lifetimes of $^1G_4$ level is found to be independent of temperature with a mean value 480 and 205 μs for the long and short decays, respectively. This implies that the quantum efficiency of these levels is also temperature independent. The decay time of the $^3F_4$ level shows a small temperature dependence. For example, the longer decay time of this level was measured to be 450 at 10 and 390 μs at 300 K.

3.2.2. *Upconversion upon* 966 nm *excitation.* Upconversion emission spectra of APbF:20 mole% YbF_3; 0.2 mole% TmF_3 sample measured in the

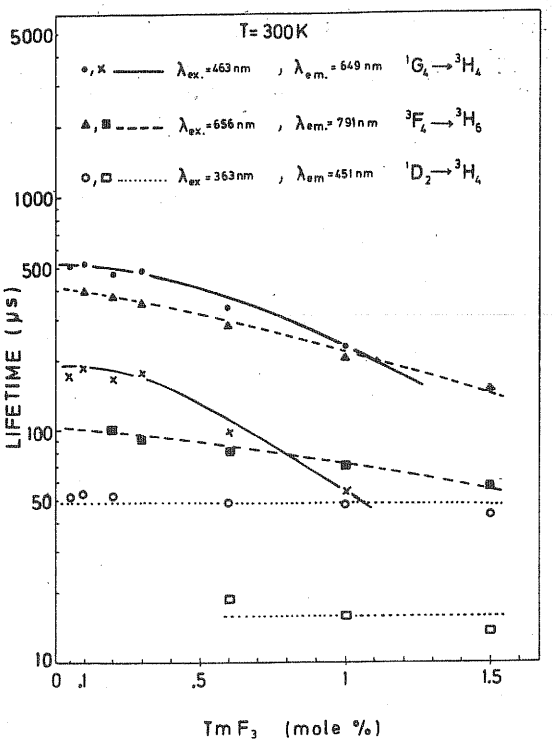

Fig. 7. Lifetime of $^1D_2$, $^1G_4$ and $^3F_4$ levels as a function of Tm^{3+} concentration at room temperature.

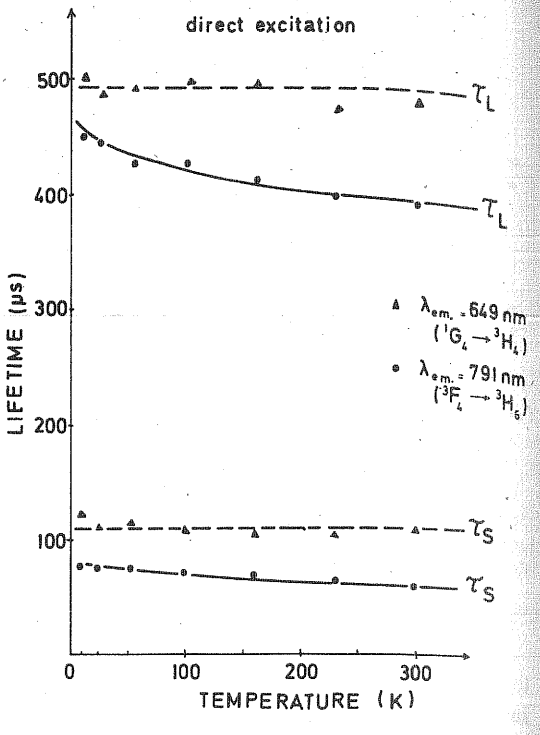

Fig. 8. Lifetime of $^1G_4$ and $^3F_4$ levels of Tm^{3+} in APbF:20 mole% YbF_3 and 0.2 mole% TmF_3 as a function of temperature upon direct excitation.

range of 440 and 830 nm at 16 and 300 K are presented in Fig. 9. The position and the shape of the emission bands are consistent with those obtained upon direct excitation of the excited levels of Tm^{3+} ions. But the intensity ratio of the 649 nm with respect to the 791 nm emission is much greater than the one measured upon i.r. excitation of $^1G_4$ level (see Figs 3 and 9). The excitation spectrum of each emission was obtained at room temperature. All the spectra correlate well with the absorption spectrum of ytterbium. Quadratic and cubic dependence on the excitation power was observed for the emissions of $^3F_4$ and $^1G_4$ levels, respectively. This indicates that the two photon and three photon absorption processes are responsible for the upconverted emissions of these levels as can be seen in Fig. 10.

Decay patterns of $^1G_4$ emission obtained upon direct and i.r. excitation are given in Fig. 11 for comparison. The decay pattern of the upconverted emission shows a rise in addition to the decay process. The time constants of the curves presented in Table 4 were measured for different concentrations of Tm^{3+} and Yb^{3+} at room temperature. The rise time becomes shorter when the concentration of Tm^{3+} increases due to energy transfer processes from Yb^{3+} to Tm^{3+}. The decay time measured upon i.r. excitation is shorter than that obtained upon direct excitation.

4. DISCUSSION

Our experimental results agree with the model for the upconversion process proposed by Auzel [17].

Table 3. Decay times of the excited levels of Tm^{3+} measured for different Tm^{3+} concentrations at room temperature. Measurements were made by exciting each level directly

Concentration (mole%)		Decay time (μs) $^1D_2$ level		$^1G_4$ level		$^3F_4$ level	
Yb	Tm	τ_{short}	τ_{long}	τ_{short}	τ_{long}	τ_{short}	τ_{long}
20	0.05	17	52	176	512	—	—
20	0.1	17	55	193	522		396
20	0.2	18	54	170	483	102	380
20	0.3	16	52	182	478	95	378
20	0.6	17	48	120	390	80	290
20	1.0	14	45	54	307	68	240
20	1.5	12	40	—	—	57	185

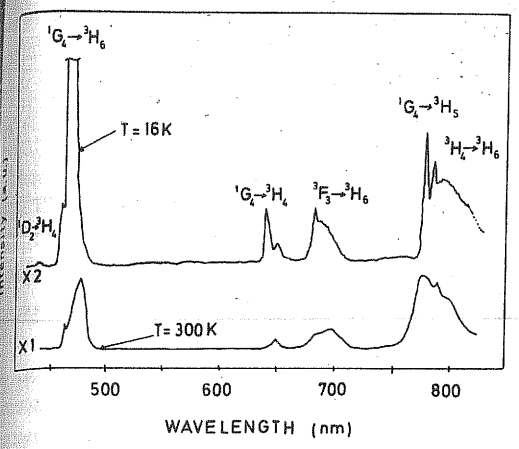

Fig. 9. Upconversion emission spectra of APbF:20 mole% PbF_3 and 0.2 mole% TmF_3 upon i.r. excitation at 966 nm (excitation was into the Yb^{3+} ions).

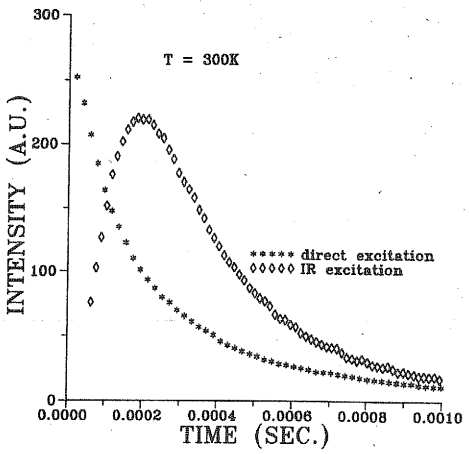

Fig. 11. Decay pattern of $^1G_4$ level obtained upon direct and i.r. excitations at room temperature.

Here a Tm^{3+} ion is excited by nonresonant energy transfer from Yb^{3+} ions and multiphonon decays in Tm. According to the energy levels of Tm^{3+} in this matrix, for each step of transfer from Yb^{3+} to Tm^{3+} phonon(s) must be given off to the host. Phonon cut-off frequency of the host was measured from the Raman spectrum and found to be 650 cm^{-1}. The energy mismatch between the levels involved in the first, second and third energy transfer processes was measured from the absorption spectra given in Fig. 1. These values are 1250, 1458 and 1666 cm^{-1}, respectively. This indicates that at least two phonons for the first two, and three phonons are released during the third transfer processes. The validity of Auzel's model was confirmed by measuring the excitation spectra and the dependence on excitation power of each upconverted emission. Shorter rise time obtained for a higher concentration of Tm also supports this model. The upconverted emission intensity for the two and three photon processes calculated using the rate equation model [18] in the case of low excitation power is proportional to the following:

$$I(791\text{ nm}) \propto \tau(791\text{ nm}) C_{D2} C_{D4} N_a N_d^2 (\sigma^D \phi)^2 \quad (5)$$

and

$$I(479\text{ nm}) \propto \tau(479\text{ nm}) C_{D2} C_{D4} C_{D5} N_a N_d^3 (\sigma^D \phi)^3, \quad (6)$$

where N_A and N_D are the total concentrations of the acceptor (Tm^{3+}) and donor (Yb^{3+}) ions, σ^D is the absorption cross-section of donor ions and ϕ is the excitation flux. The τ is the measured decay time of the level from which the upconverted emission is observed and c_{Di} is the transfer rate from donor to the ith level of acceptor.

Equations (5) and (6) show that the upconverted emission intensity or efficiency depends on the following parameters.

(i) Excitation power; according to intensity vs excitation power mesurements of emissions (see Fig. 10), the blue emission centered at 479 nm ($^1G_4 \rightarrow {}^3H_6$ transition) is due to a three sequential transfer from Yb^{3+} while the red emission centered at 791 nm (corresponding to $^3F_4 \rightarrow {}^3H_6$ transition) is the result of a two sequential transfer from Yb^{3+} ions.

(ii) Quantum yield of the emitting level; the efficiency of each upconverted emission depends

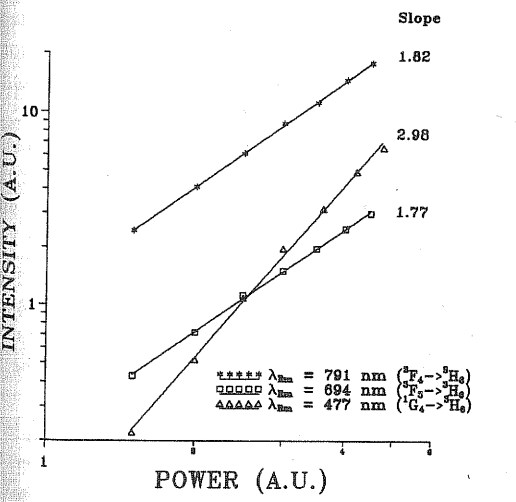

Fig. 10. Dependence on the excitation power of the upconverted emission intensities of Tm^{3+} in APbF:20 mole% PbF_3 and 0.2 mole% TmF_3 upon 996 nm excitation at room temperature.

Table 4. Rise and decay time of $^1G_4$ level measured for different concentrations of Tm^{3+} and Yb^{3+} upon i.r. excitation at room temperature

Concentration (mole%)		Time constant (μs)	
Yb	Tm	τ_{rise}	τ_{decay}
10	0.2	60	188
20	0.2	80	283
20	1.0	30	83

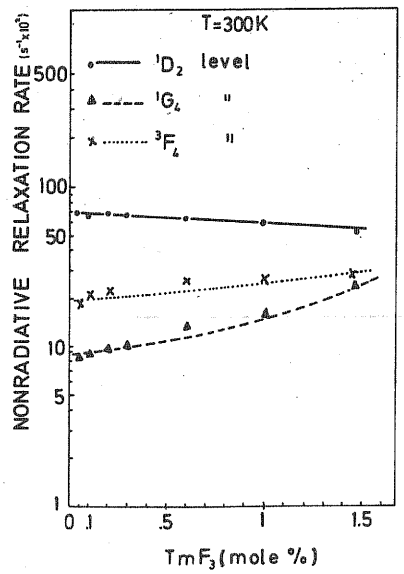

Fig. 12. Multiphonon relaxation rates of the excited levels of Tm^{3+} in APbF:20 mole% YbF_3 and 0.2 mole% TmF_3 upon direct excitation of the desired level at room temperature.

strongly on the quantum yield of the final level as well as the effective energy transfer from the intermediate levels involved in the process. The quantum yield of the final level is given as the ratio of the measured and radiative lifetimes. The measured lifetime of an excited level may be given as:

$$1/\tau = W_R + W_{MP} + W_{TE}, \qquad (7)$$

where W_R is the radiative transfer rate of the level, W_{MP} and W_{TE} are the multiphonon relaxation and the

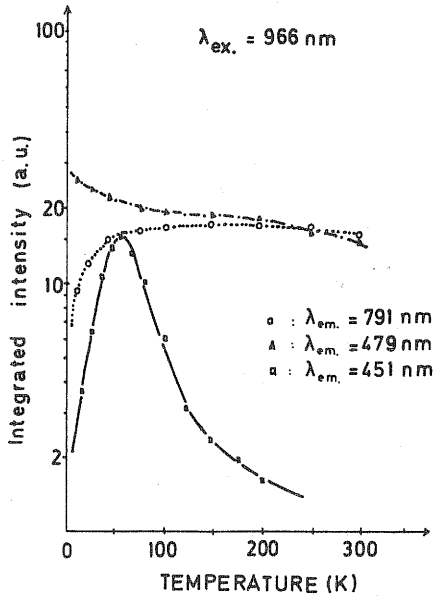

Fig. 13. Temperature dependence of some emissions observed in APbF:20 mole% YbF_3 and 0.2 mole% TmF_3 upon i.r. excitation.

Table 5. Absolute efficiencies of the upconverted emissions observed upon i.r. excitation at room temperature

Excitation power mW cm^{-2}	Emission 479 nm ($^1G_4 \rightarrow {}^3H_6$)	791 nm ($^3F_4 \rightarrow {}^3H_6$)
16.5	—	6.15×10^{-4}
20.0	5×10^{-8}	7.1×10^{-4}

energy transfer rate, respectively. The quantum yield of the level depends on the multiphonon relaxation and the energy transfer rates.

(iii) Concentration of acceptor and donor; the upconverted emission intensity depends on acceptor concentration linearly in both equations. However, the intensity of, for example, 479 nm emission starts decreasing above 0.2 mole% Tm^{3+} concentration (see Fig. 4). The quenching of the emission intensity of $^3F_4$ and $^1G_4$ levels may be due to the energy transfer to Yb^{3+} ions as well as cross-relaxation processes between Tm^{3+} ion-pairs. The $^1G_4$ emission may be quenched by four resonant ion-pair relaxation processes: $(^1G_4,{}^3H_6) \rightarrow (^3F_2,{}^3H_4)$ or $(^3H_4,{}^3F_2)$ or $(^3F_4,{}^3H_5)$ or $(^3H_5,{}^3F_4)$. Dependence of the emission intensity on the Tm^{3+} concentration shows that the cross-relaxation processes occur for Tm^{3+} concentrations higher than 0.2 mole%. The cross-relaxation process from the $^3F_4$ level is nonresonant case and corresponds to the $(^3F_4,{}^3H_6) \rightarrow (^3H_4,{}^3H_4)$. Using the radiative lifetime of each level calculated by using Judd–Ofelt theory and the longer decay time measured for the samples having different Tm^{3+} concentration in eqn (7) we obtained the total quenching rate of $^1D_2$, $^1G_4$ and $^3F_4$ levels by multiphonon relaxation and the energy transfer. The results are given in Fig. 12. The quenching of $^1G_4$ level by Tm^{3+} is slightly stronger than that of $^3F_4$ level. The quenching of $^1G_4$ emission by Yb^{3+} ions was obtained by measuring the emission intensity as a function of Yb concentration at room temperature by exciting the $^1G_4$ level directly. As can be seen from Fig. 5, the quenching of this emission due to the back transfer from $^1G_4$ level to Yb^{3+} ions is negligible for the Yb^{3+} concentrations from 2 to 25 mole%. On the other hand, the $^1D_2$ emission is quenched neither by Tm^{3+} nor by Yb^{3+} ions in the range of 0.05–1.0 and 2–25 mole% of Tm^{3+} and Yb^{3+} concentrations, respectively. This indicates that effect of the interaction between Tm^{3+}–Tm^{3+} and Tm^{3+}–Yb^{3+} on the $^1D_2$ emissions is negligible.

(iv) Transfer rate from donor to acceptor; c_{Di} terms in the equations are also important parameters for the upconversion efficiency. In the case of Tm^{3+}–Yb^{3+} all the upconverted emissions are due to nonresonant transfer processes and therefore the probability of the upconversion is related to the

)f the upconverted emissions
on at room temperature

Emission	
$^3H_6$)	791 nm ($^3F_4 \rightarrow {}^3H_6$)
	6.15×10^{-4}
	7.1×10^{-4}

ively. The quantum yield
multiphonon relaxation
es.
cceptor and donor; the
sity depends on acceptor
oth equations. However,
e, 479 nm emission starts
% Tm^{3+} concentration
of the emission intensity
due to the energy transfer
ross-relaxation processes
he $^1G_4$ emission may be
ion-pair relaxation pro-
H_4) or ($^3H_4$,$^3F_2$) or
pendence of the emission
centration shows that the
occur for Tm^{3+} concen-
le%. The cross-relaxation
is nonresonant case and
) $\rightarrow$ ($^3H_4$,$^3H_4$). Using the
level calculated by using
the longer decay time
having different Tm^{3+}
we obtained the total
and $^3F_4$ levels by multi-
energy transfer. The re-
he quenching of $^1G_4$ level
than that of $^3F_4$ level. The
y Yb^{3+} ions was obtained
intensity as a function of
temperature by exciting
n be seen from Fig. 5, the
due to the back transfer
is negligible for the Yb^{3+}
25 mole%. On the other
uenched neither by Tm^{3+}
range of 0.05–1.0 and
Yb^{3+} concentrations, re-
at effect of the interaction
Tm^{3+}–Yb^{3+} on the $^1D_2$

nor to acceptor; c_{Di} terms
important parameters for
ncy. In the case of
erted emissions are due to
esses and therefore the
ersion is related to the

ergy mismatch between the levels involved in the upconversion processes. Each mismatch leads to lower probability of back energy transfer from Tm^{3+} to Yb^{3+} than it is for the resonant case upon i.r. excitation.

The quantum efficiency of the upconverted emissions was measured by using a comparative method [3]. The efficiency of the upconverted emission is defined as:

$$\eta_u = \eta_s \frac{F_u A_s \lambda_s^{ex}}{F_s A_u \lambda_u^{ex}} \frac{n_u^2}{n_s^2}, \quad (9)$$

where η_u and η_s are the quantum yields of unknown and the standard, respectively. n_u and n_s are the refraction indexes, A is the absorbance at the excitation wavelength and F is the integrated area under the emission band and λ_{ex} is the excitation wavelength. We have used the efficiency for Tm^{3+} upconverted emissions upon i.r. excitation given in [5]. For the same emission of Tm^{3+} in two different hosts upon the same excitation conditions the efficiency of the unknown becomes:

$$\eta_u = \eta_s \frac{F_u}{F_s}. \quad (10)$$

Table 5 shows the absolute efficiencies obtained at room temperature for the divitrified APbF: 0.2 mole% TmF_3, 20 mole% YbF_3 sample upon 16.5 and 20 mW cm^{-2} excitation power. We have not observed the blue emission for the glass when the excitation power was 16.5 mW cm^{-2}. However, the efficiency of 791 nm emission due to the two photon process is measured to be 8×10^{-4} which is four times greater than that obtained by Yeh *et al.* in BZYTLTm glass [5].

Decay time of $^1G_4$ level of Tm^{3+} in APbF: 0.2 mole% TmF_3, 20 mole% YbF_3 sample is independent of temperature upon direct excitation. Therefore the multiphonon relaxation rate or the quantum yield of the level is also independent of temperature. In other words, the effect of the quantum yield of $^1G_4$ level on the temperature dependence of the upconverted blue emission is negligible. The decay time of the $^3F_4$ level shows weak dependence on temperature. This indicates that the rate of the multiphonon and the transfer processes initiating from this level is temperature-dependent and the quantum yield of this level is an important parameter for the upconversion efficiency of 791 nm emission.

5. CONCLUSION

The upconverted red and blue emissions from $^3F_4$, $^1G_4$ and $^1D_2$ levels of Tm in APbF: TmF_3, YbF_3 glasses were observed upon 966 nm excitation. An absolute efficiency for blue (479 nm) and red (791 nm) emissions was measured at room temperature by using a comparative method with a standard sample. The divitrified glass gives a higher efficiency for both emissions than the glass. This may be because more ions (Tm^{3+} and Yb^{3+}) are located in the crystalline phase in the divitrified matrix [19].

Judd–Ofelt theory was used to obtain the optical properties of Tm ions and some parameters such as the quantum yield of the final level and the branching ratio of the emissions were calculated. Blue emission, centered at 479 nm, of $^1G_4$ level has the highest branching ratio between the transitions originating from this level. The quantum yield of this level is found to be independent of temperature with a mean value of 0.56. The quantum yield of $^3F_4$ level shows a small dependence on temperature. This parameter may be more important to explain the temperature dependence of upconverted red emission than it is for the blue emission. The temperature dependence of 479 nm emission therefore is mainly due to the c_{Di} parameters which depend on the transfer mechanism between Yb^{3+} and Tm^{3+} ions.

By measuring the temperature dependence of the upconverted emissions, an optimal upconversion efficiency was obtained at 150 K for the red emission while the blue emission shows a maximum efficiency at 10 K. Two exponential lifetimes observed for levels suggest that Tm^{3+} ions in this host are not uniformly distributed. Decay time of the $^1G_4$ emission upon i.r. excitation gives a shorter value than that measured upon direct excitation. This value is between the shorter and longer decay times obtained upon the latter excitation. This indicates that the transfer from Yb^{3+} to only occur to those Tm^{3+} ions close to Yb^{3+}.

Acknowledgements—We would like to thank Ph. Goldner for his interesting discussions, M. Genotelle for preparing the samples and N. Gardant for calibrating the experimental system. This work was partially supported by the MRT contract No 501444.

REFERENCES

1. van der Ziel J. P., Van Uitert L. G., Grokiewicz W. H. and Mikuljak R. M., *J. appl. Phys.* **60**, 4262 (1986).
2. Yeh D. C., Sibley W. A., Suscavage M. and Drexhage M. G., *J. appl. Phys.* **62**, 266 (1987).
3. Tanabe S., Hirao K., Soga N. and Hanada T., SPIE 1513. *Proc. Int. Cong. Opt. Sci. Eng.* 340 (1991).
4. Shin M. D., Sibley W. A., Drexhage M. G. and Brown R. N., *Phys. Rev. B* **27**, 6635 (1983).
5. Yeh D. C., Sibley W. A. and Suscavage M., *J. appl. Phys.* **63**, 4644 (1988).
6. Ryba-Romannowski W., Golab S. and Dominiak-Dzik G., *J. Phys. Chem. Solids* **54**, 153 (1993).

7. Gurey C., Adam J. L. and Lucas J., *J. Lum.* **42,** (1988).
8. Kermaoui A., Barthou C., Denis J. P. and Blanzat B., *J. Lum.* **29,** (1984).
9. Hewes R. A., *J. Lum.* **1,** 778 (1970).
10. Judd B. R., *Phys. Rev.* **127,** 750 (1962).
11. Ofelt G. S., *J. Chem. Phys.* **37,** 511 (1962).
12. *Laser Crystals* (Edited by A. A. Kaminskii). Springer-Verlag, Berlin (1981).
13. Reisfeld R. and Eckstein Y., *J. Non-Cryst. Solids* **15,** 125 (1974).
14. Oomen E. W. J. L., *J. Lum.* **50,** 317 (1992).
15. Harinath R., Buddhudu S., Bryant F. J. and Xi Luo, *Solid State Commun.* **74,** 1147 (1990).
16. Wright J. C., *Top. Appl. Phys.* **15,** 239 (1976).
17. Auzel F., *Proc. IEEE* **61,** 758 (1973).
18. Ostermayer F. W., van der Ziel Jr. J.P., Mercos H. M., Van Uitert L. G. and Geusic J. E., *Phys. Rev. B* **3,** 2698 (1971).
19. Auzel F., Pecile P. and Morin D., *J. electrochem. Soc.* **122,** 101 (1975).